Ball-and-Chain Dimers from a Hot Fullerene Plasma

Alexandre A. Shvartsburg,[†] **Robert R. Hudgins,**[†] **Rafael Gutierrez,**[‡] **Gerd Jungnickel,**[§] **Thomas Frauenheim,**[§] **Koblar A. Jackson,**[∥] **and Martin F. Jarrold*,**[†]

Department of Chemistry, Northwestern University, 2145 Sheridan Road, Evanston, Illinois 60208, Theoretische Physik, Technische Universität Chemnitz, D-09107 Chemnitz, Germany, Theoretische Physik, Universität−GH Paderborn, D-33098, Germany, and Department of Physics, Central Michigan University, Mt. Pleasant, Michigan 48859

The laser desorption of C_k (k = 60 and 70) fullerene is known to produce a broad distribution of cluster sizes strongly peaking around the integer multiples of original fullerene mass. The "exact dimers" (C_n clusters with n = 2k) and species with slightly fewer atoms (n even) have been characterized previously as fully coalesced large single-shell fullerenes and [2 + 2] cycloadducts. Presently, we investigate the species encountered on the high-mass sides of exact dimers, that is, the clusters with n > 2k (n even), using high-resolution ion mobility measurements. Specifically, the drift time distributions for C_n^+ and C_n^- with n = 122−128, 132−136, and 142−146 have been obtained and compared with the results of trajectory calculations for various trial geometries optimized using the density functional tight binding and semiempirical (AM1) calculations. We find that, besides the normal near-spherical fullerenes and [2 + 2] cycloadducts, these species assume the "ball-and-chain" structures consisting of two fullerene cages (not necessarily those of the original material) connected by chains up to eight atoms long. C_{122} and C_{132} cations and anions also reveal a substantial abundance of isomers where the C−C unit is sandwiched between the two fullerenes. Taken in conjunction with earlier findings for smaller fullerene dimers, presently reported results have allowed us to develop a comprehensive model for the chemical reactions occurring in the hot fullerene plasma.

Introduction

Upon laser desorption, C_{60} and C_{70} fullerenes yield clusters with masses at integer multiples of 60 or 70 carbon atoms.[1−19] The structure of these species has been the object of much attention, particularly in view of a large diversity of fullerene oligomer and polymer phases synthesized in the solid state (pertinent literature has been reviewed in refs 18 and 19). Dimers and trimers of C_{60} and C_{70} have been used to computationally model the intermolecular links in bulk polymers, so the structure of these clusters has been extensively studied by theory (see refs 18 and 19). Mixed $C_{60} \cdot C_{70}$ dimers have also been optimized.[20] Calculations indicate that all these are joined via a [2 + 2] cycloaddition (at least in the neutral state), and in fact so are the C_{60} cages in all solid-state polymer phases characterized so far. The C_{60} dimer that has recently been synthesized and isolated by chemical means is also a [2 + 2] cycloadduct.[21,22] In comparison, there has been little experimental research on the gas-phase clusters of fullerenes. Early work has produced some indirect arguments in favor of either individual C_{60} or C_{70} cages joined by generic cross-links[1−6,10,11] or a complete coalescence into giant single-shell fullerenes.[7,8] The laser desorption of fullerenes normally generates clusters not only at integer multiples of the monomer mass but in fairly broad mass envelopes around those multiples, with peaks at even numbers of carbon atoms. Actually, the features at exact multiples are often not the most prominent in each envelope. There had been a few theoretical suggestions[10,16] about the

geometries of clusters with other masses (such as C_{116}, C_{118}, C_{136}, and C_{138}), but none has had any experimental support.

We have recently used ion mobility measurements[17−19] to investigate the products of laser desorption of C_{60} and C_{70} with masses equal to or less than 2 × 720 and 2 × 840 amu, respectively, that is, clusters encountered on the left sides of the mass envelopes. Specifically, C_n cations and anions with n = 112, 114, 116, 118, 120, 136, 138, and 140 have been studied, as well as C_{130}^+ and C_{130}^- produced from the mixed C_{60}/C_{70} sample. We have found that all these clusters exhibit two structural families: single-wall fullerenes (mostly near-spherical with an admixture of elongated fullerenes) and [2 + 2] cycloadducts.[18,19] The relative yield of fullerenes increases with increasing laser power in the source[18] or injection energy in the drift tube,[17] which indicates the annealing of cycloadducts into fullerenes that are lower in energy by over 20 eV.[23] Higher laser power also causes the conversion of tubular fullerene cages into lower-energy more spherical ones.[18,19] The quadruply bound and other multiply bound adducts previously proposed[10,16] for C_{116} and C_{118} have not been observed in these experiments. The conclusion is that the clusters with masses less than the exact multiples of the original fullerene mass are formed by coalescence of dissociation products.[19] That is, hot laser-desorbed fullerenes cool by evaporating one or more C_2 units and then add to other cages, as suggested by Hertel and collaborators.[13] The fact that the only products of fullerene bimolecular reaction are the [2 + 2] cycloadducts and giant fullerenes finds an excellent explanation[19] when one considers the potential energy of the $C_{60} \cdot C_{60}$ system as it proceeds along the coalescence pathway from separated cages to the lowest-energy C_{120} T_d fullerene.[23]

[†] Northwestern University.
[‡] Technische Universität Chemnitz.
[§] Universität−GH Paderborn.
[∥] Central Michigan University.

In this contribution, we focus on the clusters with masses higher than the integer multiples of the starting fullerene mass. It has been hypothesized[13] that these arise from the addition of C_2 units to preformed dimers of original fullerenes (C_{60} or C_{70}) or their smaller fragments resulting from the laser-shrinking. On the other hand, Osterodt and Vogtle,[24] Strongin and co-workers,[25] and Dragoe et al.[26] have isolated the bicyclopropyl-idene C_{122} consisting of C_{60} fullerenes joined by a ($>C=C<$) bridge with sp^2-hybridized C atoms added across C_{60} bonds shared by two hexagons (66 bonds). This moiety is produced by the dimerization of a C_{61} intermediate with a lone electron pair on propyle ring formed by the addition of a carbon atom across a 66 bond of C_{60}. Such "ball-and-chain" geometries could be constructed for clusters with $n > 122$ using longer chains and/or larger fullerenes. Similar structures with C_{60} cages joined by carbon chains of variable length have been conjectured by Martin and co-workers[27] for the C_{60} oligomers produced by covaporization of graphite and C_{60}. To elucidate the nature of species on the right sides of mass envelopes generated by laser desorption of fullerene, we have performed high-resolution ion mobility measurements on the C_n cations and anions for $n = 122-128$, $132-136$, and $142-146$ (n even).

Experimental Methods

The experiments were performed using the high-resolution ion mobility apparatus described in detail elsewhere.[28] Briefly, the apparatus consists of a source region directly coupled to a 63 cm long drift tube. Both are filled with He buffer gas at a pressure of about 500 Torr at a temperature of 25 °C. The cluster ions are generated by pulsed 308 nm laser desorption of C_{60} or C_{60}/C_{70} fullerene films deposited on a rotating and translating copper rod. After formation, the ions are guided by electric fields through a small aperture in the ion gate that separates the source from the drift tube. The ion gate is installed in order to prevent neutral species from entering the drift tube. This is achieved by arranging the helium flow through the gate from the drift tube into the source, while an electric field pulls the ions upstream. The ions then travel along the drift tube under the influence of a uniform electric field (160 V/cm) generated by a stack of isolated rings. Ions exiting the drift tube through a small aperture are mass-selected by a quadrupole mass spectrometer and detected by an off-axis collision dynode and dual microchannel plates. Drift time distributions are recorded with a multichannel scaler triggered by the laser pulse.

Results

The drift time distributions measured for C_{122}, C_{124}, and C_{126} cations and anions are presented in Figure 1. The scales on top show the inverse mobilities, which are proportional to the drift times. This is a customary way to express ion mobility data, since the inverse mobilities are also proportional to the orientationally averaged collision integrals. The distributions for $n = 122-126$ and 128 (not shown) differ in two significant ways from those observed for both cations and anions of either the "exact" dimers of original fullerenes[18] (C_{120} and C_{140}) or lighter clusters in the same mass envelopes.[19] First, the scans for both charge states reveal more than the two peaks encountered[18,19] for $n = 112-120$ (n even) or $n = 130$. As discussed below, the first and second peaks from the left correspond respectively to the near-spherical fullerene cages and [2 + 2] cycloadducts found for smaller clusters.[18,19] The difference is in the new features, typically smaller than either of those two, appearing at the longer drift times from the second leftmost peak. In the progression from C_{122} to C_{128}, the separation from

[2 + 2] cycloadducts to the end of a series monotonically increases, while the intensity of new features decreases, reducing to a trace for C_{128}. Second, the new peaks for cations and anions of $n = 122-126$ are quite different, whereas the drift time distributions for $n = 112-120$ are totally independent of the charge state. For example, the anions for all three sizes have two or three "extra" major peaks whereas the cations have only one. The cumulative abundance of novel features is uniformly smaller for cations.

The data for C_{132}, C_{134}, and C_{136} are overall similar to those for $n = 122-126$. The relative abundance of new isomers again decreases on going from $n = 132$ to 134 to 136 but is always lower than for the corresponding C_{n-10} with the same charge. Unlike the situation with $n = 124$, there is hardly a significant difference between C_{134}^- and C_{134}^+ (Figure 2); both resemble C_{124}^-. The new features for $n = 136$ could be identified for anion only, perhaps owing to insufficient signal. In fact, the "extra" peaks for C_{136}^- (Figure 2) are so minor ($\sim$0.1% fractional abundance) that we had missed them previously.[19] For C_{142}, C_{144}, and C_{146} cations and anions, we have observed the standard fullerene and [2 + 2] cycloadduct peaks. The latter normally end in lengthy tails gradually decaying to the right. These may include unresolved features analogous to those found for $n = 122-126$ and $132-136$.

The relative abundances of novel features described above are sensitive to the source and laser conditions.

Mobility Calculations

To assign the features observed in drift time distributions to specific geometries, one has to evaluate the mobilities for a number of plausible candidates. All our experiments are performed in the low drift field limit where the mobility is independent of the field and given by[29]

$$K = \frac{(18\pi)^{1/2}}{16}\left[\frac{1}{m} + \frac{1}{m_b}\right]^{1/2} \frac{ze}{(k_BT)^{1/2}} \frac{1}{\Omega_{avg}^{(1,1)}} \frac{1}{N}$$

where m and m_b are respectively the masses of the ion and the buffer gas atom, T and N are the buffer gas temperature and number density, ze is the ionic charge, and $\Omega_{avg}^{(1,1)}$ is the orientationally averaged collision integral.

We determine $\Omega_{avg}^{(1,1)}$ by propagating classical trajectories of He atoms in a realistic He/cluster intermolecular potential.[30] A function of the scattering angle is averaged over the impact parameter and collision geometry assuming the free rotation of drifting cluster, which yields the momentum transfer cross section. Integrating this quantity over the Maxwellian distribution of relative velocities between the buffer gas atom and the ion produces $\Omega_{avg}^{(1,1)}$. The He/cluster potential is modeled as a sum of pairwise Lennard-Jones interactions plus a charge-induced dipole term.[31] In our previous work on the fullerenes and their adducts,[18,19,30,31] an ionic charge uniformly delocalized over all cluster atoms has been assumed. However, the latest research has demonstrated that the ion mobility may be materially affected by localization of charge on certain cluster atoms.[31,32] So now we have employed the self-consistent Mulliken charge distributions produced by DFTB calculations (see below). Within the computational error margin ($\sim$0.2%), the mobilities for species considered here are not influenced by this improvement. This is in part because the deviations from uniform charge delocalization are smaller in any of the fullerene dimers than in structures including a primary carbon such as

Dimers from Fullerene

J. Phys. Chem. A, Vol. 103, No. 27, 1999 **5277**
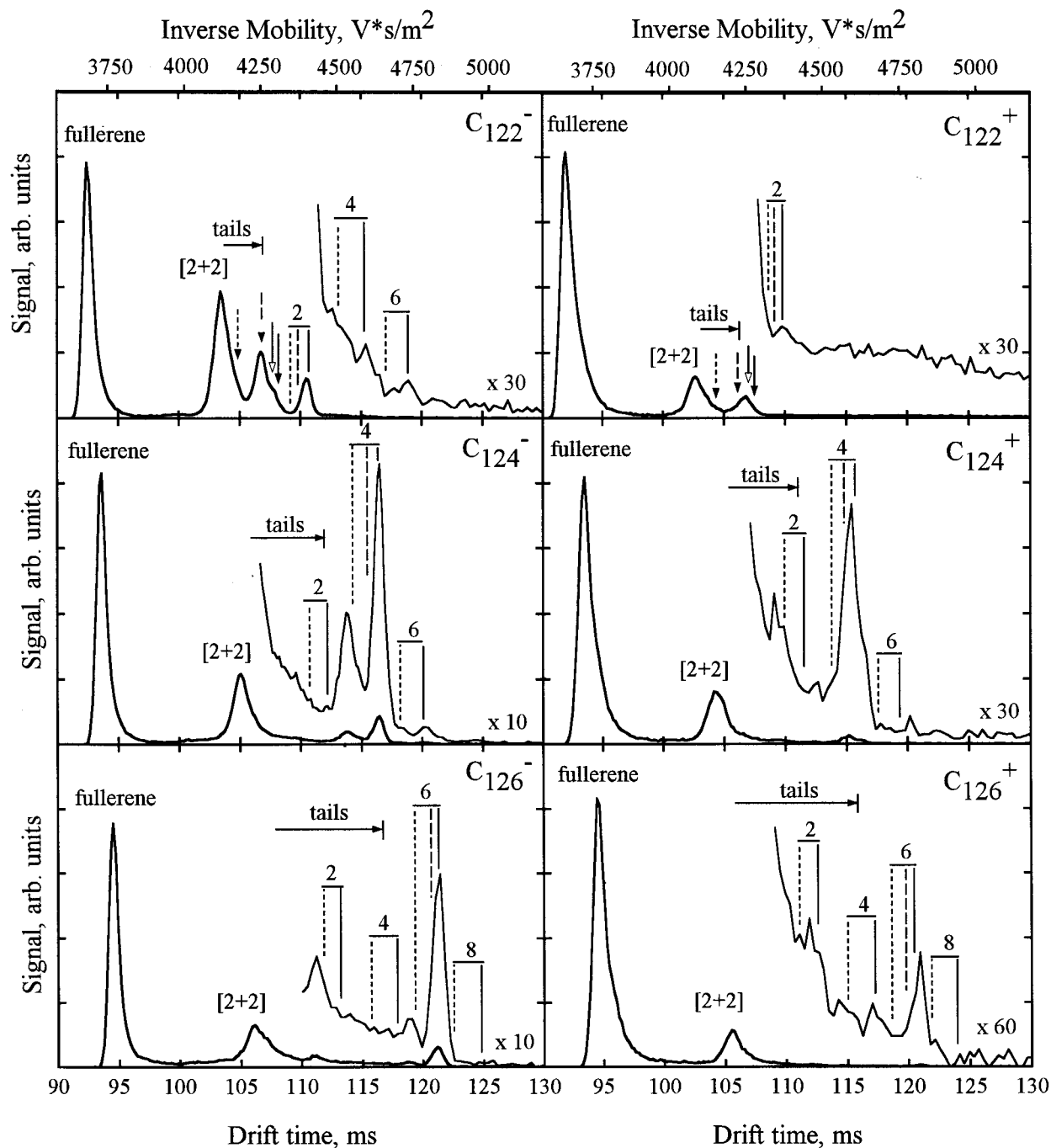
Figure 1. Drift time distributions for the C_{122}, C_{124}, and C_{126} cations and anions. Scales on the top of figure indicate the inverse reduced mobilities. The drift times calculated for ball-and-chain dimer geometries discussed in the text are superimposed. Dotted, dashed, and solid bars are for the open-56 sp^2, closed-66 sp^2, and sp isomers, respectively. The number of carbons in the chains is given above. Horizontal "tails" arrows correspond to the ranges of mobilities for regular [2 + 2] cycloadducts with side chains ("tailed dimers"). The vertical arrows for C_{122}^- and C_{122}^+ mark the singly bonded $C_{60} \cdot C_{62}$ dimer (dotted), "benzene"-link structure (dashed), and the double [2 + 2] geometries (solid). For the latter, the empty and filled arrowheads correspond to the "open" and "closed" isomers, respectively.

chains[31] or chains attached to rings[32] and in part simply because of large cluster size ($n \approx 120-140$ compared with $n \leq 20$ for the chains[31] and new monocyclic rings[32]). And in fact, the approximation of uniform charge delocalization has provided extremely accurate values for the mobilities of fullerene dimers.[18,19,31]

Cluster Geometries

Computational Method. All candidate geometries for mobility calculations have been optimized using the recently devel-

oped self-consistent charge density functional tight binding method (DFTB).[33] This enhances the earlier formalism[34] by adding the self-consistent charge capability, which is of particular importance for the charged clusters. The basic model[33] has been extensively validated in the treatment of fullerenes[35-37] and their dimers.[20,38,39] To ascertain the independence of computed mobilities of the specific method of geometry optimization, we have recalculated selected structures for the neutrals using the semiempirical AM1 functional known for its robust performance for fullerene dimers.[10,16,19,23,40-44] In all cases considered, the collision integrals evaluated for AM1 geometries
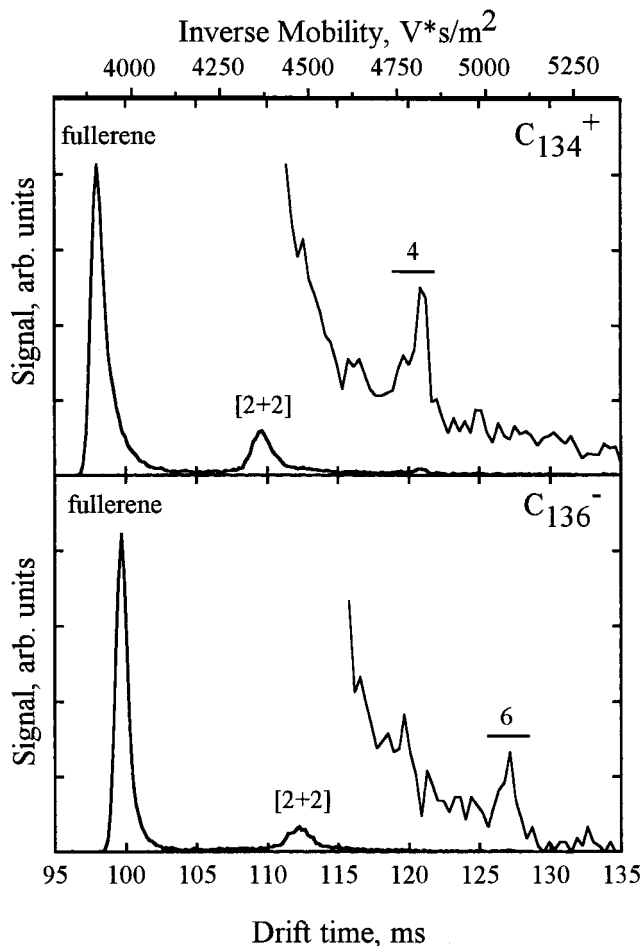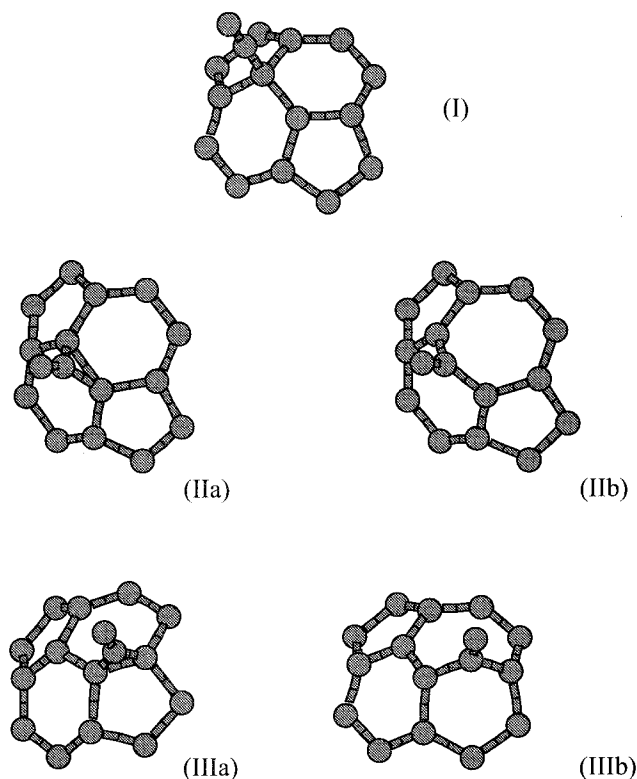
Figure 2. Drift time distributions for C_{134}^+ and C_{136}^-. Scale on the top indicates the inverse reduced mobilities.
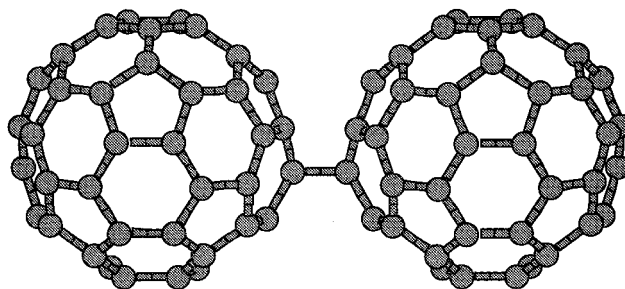

Figure 3. Five conceivable types of chain$-C_{60}$ joint: sp (I), closed-66 sp^2 (IIa), open-66 sp^2 (IIb), closed-56 sp^2 (IIIa), and open-56 sp^2 (IIIb).

Figure 4. Singly bonded C_{60} dimer.

are within -0.4 to 0.0% of those for the DFTB geometries. All findings below are for the DFTB structures unless stated otherwise.

Ball-and-Chain Dimers. As apparent from Figures 1 and 2, the new features to be assigned for $n = 122-128$ and $132-136$ have larger cross sections than the [2 + 2] cycloadducts. Further, in both cases the inverse mobilities for the rightmost major peak increase as a function of n by approximately 100 V s m^{-2} per atom in either cations or anions. This increase is much swifter than ~ 20 V s m^{-2} atom^{-1} for the [2 + 2] cycloadducts and fullerenes. The inverse mobilities of linear carbon chain cations and anions also increase by $\sim$100 V s m^{-2} atom^{-1},[31,45,46] and this is the only other structural family of carbon clusters with mobilities that strongly depend on the cluster size. This and the recent reports[25,26] of isolated C_{122} consisting of two C_{60} fullerenes linked by a C_2 chain have inspired us to test if the new peaks for $n = 122-128$, $132-136$ could be due to the ball-and-chain dimers of C_{60} and $C_{60} + C_{70}$.

Ball-and-chain dimers could be classified on the basis of the nature of chain-to-fullerene joints. There are three basic options (Figure 3): (I) "sp addition" with a single bond connecting an sp-hybridized chain to a fullerene atom, (II) "closed" sp^2 addition with an sp^2-hybridized terminal atom of a chain added across an intact fullerene bond forming a cyclopropylidene ring, and (III) "open" sp^2 addition differing from option II in that the fullerene bond in that ring is severed. Options II and III have been considered[25,26] for C_{122}; the structure actually isolated is that from option II. Option I has not been mentioned previously, but it is a generalization of the singly bonded C_{60} dimer (Figure

4) with two sp^3-carbons extensively discussed in the literature.[47] Options II and III allow for the regioisomers with different addition sites. So five types of chain-to-C_{60} joints could be made: one for option I because all C_{60} atoms are equivalent and two for options II and III each, one involving a 66 and another a 56 bond of the fullerene (Figure 3). For dimers, the joints at opposite chain ends could belong to different types. Also, both type III joints could be linked with pentagons of two fullerenes on the same side of the bridge (56/56) or on the opposite sides (56/65). Hence, 18 distinct ball-and-chain dimers involving two C_{60} units and a specific chain could exist.

First, we have optimized the dimers with both joints of the same type for neutrals, cations, and anions of $C_{122}-C_{128}$ (see Figure 5 for depictions). The sp^2 addition at both 56 and 66 bonds severs them, producing open dimers (Figure 5c,d), which relieves the strain on the three-membered rings. For the 56 case, this finding agrees with our AM1 modeling and other semiempirical calculations on methanofullerenes.[24] However, the NMR data[25] indicate that the 66 hinge bonds are retained in C_{122} neutral (such as in Figure 5b). So we have optimized the closed-66 sp^2 dimer neutrals using AM1, which does not rupture[24] the

Dimers from Fullerene

J. Phys. Chem. A, Vol. 103, No. 27, 1999 **5279**
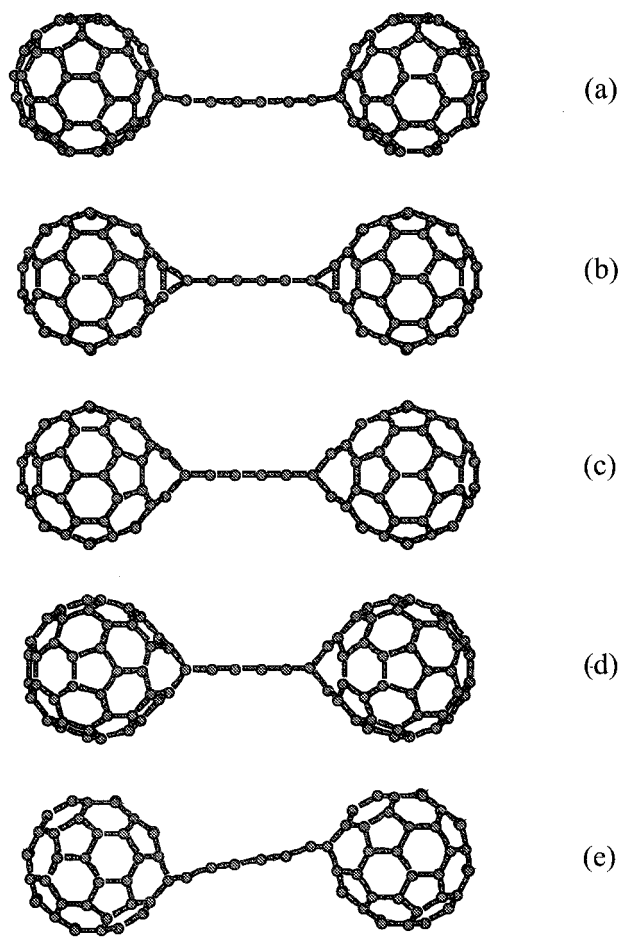
Figure 5. C_{126} ball-and-chain dimer isomers: sp (a), closed-66 sp^2 (b), open-66 sp^2 (c), and open-56 sp^2 (d); (e) shows a typical distorted conformation of (d).

TABLE 1: Energies for the sp (I) and sp^2 (IIa, the Closed-66; IIb, the Open-66; IIIb, the Open-56) Ball-and-Chain Geometries of $C_{60}-Chain-C_{60}$ Relative to the Lowest Energy Isomer[a]

geometry	cation	neutral		anion
	DFTB	DFTB	AM1	DFTB
C_{122}, I	0.63 (2.66)	1.40 (1.22)	3.42	0.66 (2.04)
C_{122}, IIa			1.00	
C_{122}, IIb	0.38 (2.91)	0.46 (2.16)	1.26 (3.52)	0.36 (2.64)
C_{122}, IIIb	0.00 (3.25)	0.00 (2.61)	0.00 (4.15)	0.00 (2.89)
C_{124}, I	0.33 (2.88)	0.92 (1.37)	3.32	0.17 (2.29)
C_{124}, IIa			0.97	
C_{124}, IIb	0.66 (2.52)	0.48 (1.83)	1.26	0.46 (1.92)
C_{124}, IIIb	0.00 (2.89)	0.00 (2.09)	0.00 (3.75)	0.00 (2.27)
C_{126}, I	0.20 (3.06)	0.68 (1.82)	3.09	0.00 (1.83)
C_{126}, IIa			0.95	
C_{126}, IIb	0.75 (2.23)	0.52 (1.63)	1.26	0.57 (1.58)
C_{126}, IIIb	0.00 (2.66)	0.00 (1.93)	0.00 (3.64)	0.02 (2.01)
C_{128}, I	0.13 (2.93)	0.52 (1.63)	2.86	0.00 (1.72)
C_{128}, IIa			0.95	
C_{128}, IIb	0.68 (2.20)	0.54 (1.53)	1.26	0.75 (1.37)
C_{128}, IIIb	0.00 (2.66)	0.00 (1.73)	0.00 (3.60)	0.09 (1.90)

[a] The dissociation energies along the lowest pathways are given in parentheses.

66 bonds in C_{122}. We have found this to be true for all chain lengths, although the open isomers remain as distinct local minima.

The relative energies of sp, 66 sp^2, and open-56 sp^2 dimers are presented in Table 1. Between the sp^2 adducts, those formed at the 56-bond are lower in energy for all chain lengths and charge states. (The 56/56 and 56/65 dimers are degenerate as they are for the [2 + 2] cycloadducts.[48]) For neutrals, the difference is almost constant at ~0.5 eV. For cations and particularly anions, it increases from ~0.4 to ~0.7 eV with increasing chain length. The sp geometry in any charge state is quite unfavorable for C_{122} (even compared with the open-66 sp^2) but quickly becomes better for longer chains. The competition between sp and sp^2 dimers is strongly influenced by the cluster charge. For anions, the sp isomer overtakes the 56 sp^2 adduct at $n = 126$ and is lower in energy for $n = 128$, while for cations and neutrals the crossover does not occur over the investigated size range. However, the sp dimer is preferable to the open-66 sp^2 one for cations with $n > 122$ and for neutrals with $n > 128$. The reason for anions favoring the sp isomers may be that both chain ends in them have almost primary carbons that are ideal for the localization of negative charge. The energy ordering of dimer families in AM1 (for all $C_{122}-C_{128}$ neutrals sp > open-66 sp^2 > closed-66 sp^2 > open-56 sp^2) and PM3[24] qualitatively agrees with the DFTB results, but the spreads in semiempirical calculation are substantially larger and less size-dependent. AM1 supports the trend for sp geometries to become more favorable for longer chains.

We have also considered mixed dimers where the chain joints to two C_{60} units are not identical. Calculations indicate that the dimers in all three charge states involving an sp and an sp^2 joint are seriously destabilized in comparison to those with either type on both ends, apparently because neither polyynic nor cumulenic bonding can propagate through the chain correctly. (As one would expect, in all charge states the penalty for this sp/sp^2 mix in comparison with the average of purely sp and sp^2 dimers decreases with increasing chain length. It varies from 1−1.3 eV for C_{124} to 0.7−1.2 eV for C_{128}.) The energies of mixed 56/66 sp^2 dimers appear to be between those for purely 56 and 66 in all charge states, similar to the case of [2 + 2] cycloadducts.[40,48]

The interfullerene bridge does not have to lie on the center-to-center axis of C_{60} units. Calculations indicate that the ball-and-chain dimers are quite flexible; cages swivel almost freely on the hinge bonds in sp^2 isomers or on the quadruply coordinated atom in sp ones within a wide range of angles. In fact, most distorted conformations (example in Figure 5e) are lower in energy by up to 0.3 eV. It may be beneficial overall to bring two highly polarizable C_{60} units closer together despite increasing local strain in the chain−fullerene joints. The distortions tend to be greater for the 56 sp^2 dimers. This is presumably because the inequivalent (pentagon and hexagon) rings on the opposite sides of the bridge distort it from normality to the cage surface.

Stability of Ball-and-Chain Dimers. To exclude the unphysical cluster geometries whose computed mobilities could coincidentally match the measurements, one has to ensure that all proposed structures are sufficiently stable to dissociation along any conceivable pathway.[49] We have verified this by optimizing unattached carbon chains and "tadpoles" consisting of chains linked to C_{60} fullerene exactly as in the dissociating dimer, for cations, anions, and neutrals. This has allowed us to rank all pathways for the breakdown of a particular dimer. We have found that the lowest ones always involve the severance of one chain−C_{60} joint. Fragmentation into two tadpoles or two C_{60} fullerenes and a chain requires much higher energies. For dimer anions, the electrons naturally reside on the tadpoles, since they have primary carbons. For cations, the energetic difference between charging tadpoles and fullerenes is slight. The prefer-

(a)

(b)
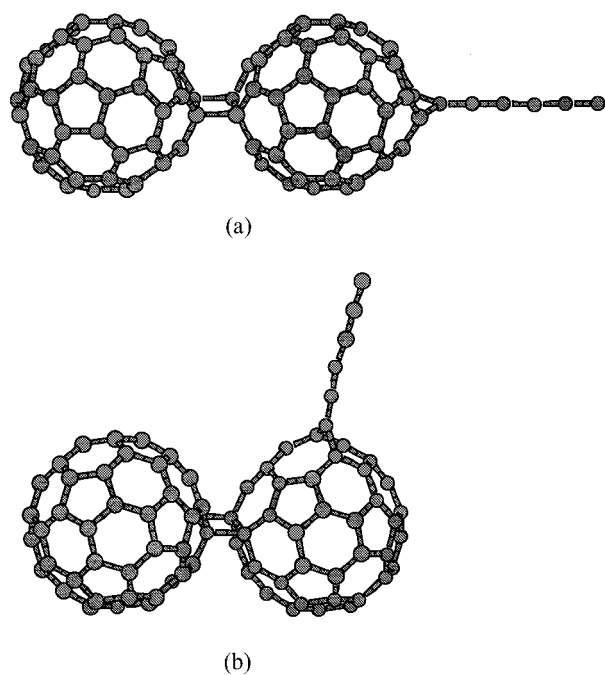
Figure 6. C_{126} "tailed" dimers: "para" isomer (a) and a geometry with lower cross section (b).

ence is usually for tadpoles to be charged because they have a quaternary carbon.

The dissociation energies calculated for the sp and sp^2 dimers in all charge states are listed in Table 1. The values for cations are particularly high because neither tadpole nor C_{60} cations are favorable (tadpoles are good for anions and C_{60} for the neutrals). The dissociation energies also decrease in all cases with increasing chain length; however, they are substantial even for $n = 128$. To put the numbers in perspective, we calculate the well-known [2 + 2] cycloadduct to be bound by 1.2 eV for $(C_{60})_2^+$, 0.6 eV for $(C_{60})_2$, and 1.0 eV for $(C_{60})_2^-$. Of course, there is a barrier to the reverse association of two C_{60}, so the activation energies for dissociation of C_{60} dimers are higher than those. In fact, both measurements[17,50] and calculations[38] produce values in the vicinity of 1.5 eV for either neutral or cation. The addition of a tadpole dangling bond to a fullerene must involve only a small activation energy if any, so the barriers to dissociation of ball-and-chain dimers should not noticeably exceed the values in Table 1. Still they are above 1.5 eV for all cations and anions, which makes both sp and all sp^2 ball-and-chain dimer ions viable under our experimental conditions. AM1 also shows smaller dissociation energies for longer chains, but the absolute values are systematically larger than the DFTB ones for all sizes. This is hardly surprising, since all semiempirical methods substantially overestimate the binding energy of the C_{60} dimer.[47,51]

Tailed Dimers. In principle, the chain in a "dimer" should not necessarily link the two fullerenes. They could be bound directly via the usual [2 + 2] cycloaddition, with a chain attached to one of them elsewhere (Figure 6). A large number of isomers of this sort could form for each chain−fullerene joint type, and we obviously could not optimize all of these. Fortunately, sample calculations show that the energy of these dimers is practically independent (within 0.1 eV) of the relative positions of the sites of [2 + 2] and chain additions, of course as long as the chain stays away from the other C_{60}. From the viewpoint of mobility, the addition of a chain opposite the [2 + 2] link (Figure 6a) maximizes the cross section. Chains added at other sites (for example, Figure 6b) result in smaller cross
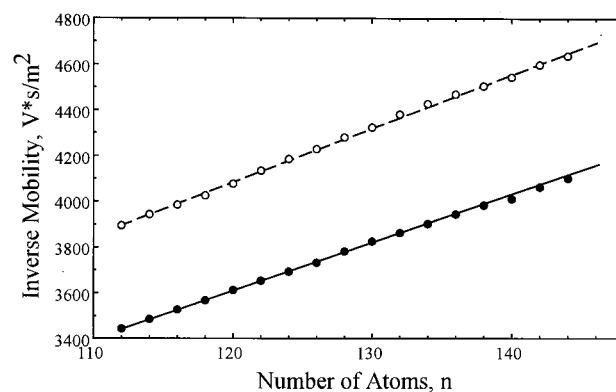
Figure 7. Inverse mobilities measured for the fullerene cage (●) and dimer (○) isomers of C_n^- with $n = 112−146$. Lines are to guide the eye. The plot for cations is similar except all values are smaller by less than 1%.

sections that are limited from below by that for the [2 + 2] $(C_{60})_2$ without a chain. So we have focused on the adducts with the chain and C_{60} cage added "para" to each other.

One would expect the energy of a tailed dimer to be above that of the ball-and-chain isomer in the same charge state by the dissociation energy of the latter less the energy recovered by [2 + 2] cycloaddition. Calculations prove this, with the resulting values coming within 0.2 eV of the above expectation. Hence, the dissociation energies of tailed dimers are close to those of the normal [2 + 2] cycloadducts, and these dimers would also be stable in our experiments.

Structural Assignments

We have verified the nature of the two leftmost peaks by plotting their mobilities as a function of cluster size.[19] The values for $n = 122−128$, 132−136, and 142−146 all fall on the two straight lines connecting the data measured for the two peaks observed for $n = 116−120$, 130, and 140 (Figure 7). Those clusters have previously been assigned as the near-spherical fullerene cages and [2 + 2] cycloadducts by comparison with calculations for the optimized geometries.[18,19] Also, the mobilities for fullerene cations measured here equal those for fullerenes produced by the laser vaporization of graphite.[52]

Ball-and-Chain Dimers. The collision integral for a fullerene dimer is mostly determined by the center-to-center distance between the C_{60} units.[18,19] So the sp ball-and-chain dimers have larger calculated inverse mobilities than all sp^2 ones. Among the sp^2 dimers, the open-66 adducts are larger than open-56 ones primarily because the interfullerene bridges in the former are nearer the center-to-center axes. The closed hinge bonds in 66 isomers further increase the intercenter distance of two C_{60} cages and thus the cross section. Hence, the drift times computed for dimers with a particular chain length are bracketed by the open-56 sp^2 adducts on the short side and sp isomers on the long side. Both open- and closed-66 sp^2 adducts are always within this range. The drift times for tailed dimer isomers similarly increase from the open-56 sp^2 to open-66 sp^2 to closed-66 sp^2 to sp. The ranges of drift times for the tailed dimers are significantly to the left of that for ball-and-chain isomers, the separation increasing for longer chains. Calculated mobilities[53] are overlayed on the measured drift time distributions in Figure 1. For all $n = 122−128$ cations and anions, the mobilities computed for the sp ($C_{60}−C_{(n−120)}$ chain−C_{60}) geometries are in an excellent agreement with the rightmost major peaks. The match for closed-66 sp^2 geometries such as that isolated[25] for C_{122} is slightly worse, but the discrepancy is small and these

Dimers from Fullerene

J. Phys. Chem. A, Vol. 103, No. 27, 1999 **5281**

structures could not be ruled out. For C_{124}^- and C_{126}^-, a smaller feature immediately leftward of that peak matches the calculations for open-56 sp^2 dimers.[56] The data for cations show no features in this position. We point out that neither of the two peaks could be due to the tailed dimers for any size.

The data for C_{124}^+, C_{126}^+, and C_{126}^- exhibit one or more minor features between the [2 + 2] cycloadducts and ball-and−chain dimers described above. The mobilities of these features are mostly within the ranges calculated for tailed dimers. It is nonetheless unlikely that the observed peaks are due to these geometries. This is because numerous tailed dimer isomers span a fairly wide range of cross sections and there is no thermodynamic or kinetic reason for any one of these structures to be preferred to the others. So these dimers may give raise to the gradually decaying tails on the right sides of [2 + 2] cycloadducts apparent for all cations and anions with $n = 124-146$ but hardly to any resolved features in the same range. However, ball-and-chain dimers do not need to be exclusive to C_{60} and not other fullerenes. For example, analogous geometries could involve both C_k ($k > 60$) fullerenes produced in plasma by incorporation of C_2 units shed by C_{60} upon laser heating into other cages and C_k ($k < 60$) fullerenes resulting from this shedding. Both are clearly present in substantial abundance, else the [2 + 2] cycloadducts for C_n ($n \neq 120$) cations and anions could not be observed. Owing to the low symmetry of fullerenes other than C_{60}, the number of distinct sites for either sp or sp^2 addition of a chain is large enough to render the detailed consideration impractical. However, the mobilities measured for [2 + 2] cycloadduct isomers in the $n \approx 110-140$ size range for either cations or anions change on going from C_n to C_{n+2} by nearly the same absolute amounts as those for the fullerene cages from C_{n-60} to C_{n-58}. So, as long as $k_1 \approx 60 \approx k_2$, one could accurately approximate the cross section of a generic $(C_{k1}-chain-C_{k2})$ ion by that for $(C_{60}-chain-C_{60})$ homologue in the same charge state plus the differences between the cross sections of C_{k1} and C_{60}, and C_{k2} and C_{60}. Using the measurements for C_{62} and C_{64} cations and anions, we have estimated the mobilities for geometries constructed by connecting them to C_{60} by two- and four-atom chains. By inspection of Figure 1, the minor peaks for C_{124}^+, C_{126}^+, and C_{126}^- are in a good agreement with the ball-and-chain dimers where the C−C unit links C_{62} or C_{64} to C_{60}. It is not necessary for these dimers to involve even one C_{60}. For example, the mobilities estimated for $(C_{58}-chain-C_{64})$ and $(C_{60}-chain-C_{62})$ isomers are close enough to render them indistinguishable in our experiments. For C_{122}^- and C_{124}^-, minor features are also observed at drift times longer than those for the major peaks assigned to $(C_{60}-C-C-C_{60})$ and $(C_{60}-C-C-C-C-C_{60})$ geometries, respectively. As indicated in Figure 1, these are in a good agreement with the mobilities for sp dimers involving longer chains and smaller cages estimated using the measured or calculated mobilities[19] for C_{56} and C_{58} ions as just described. This means that the features assigned above as $(C_{60}-chain-C_{60})$ may also include the contributions from $(C_{58}-chain-C_{62})$, etc.
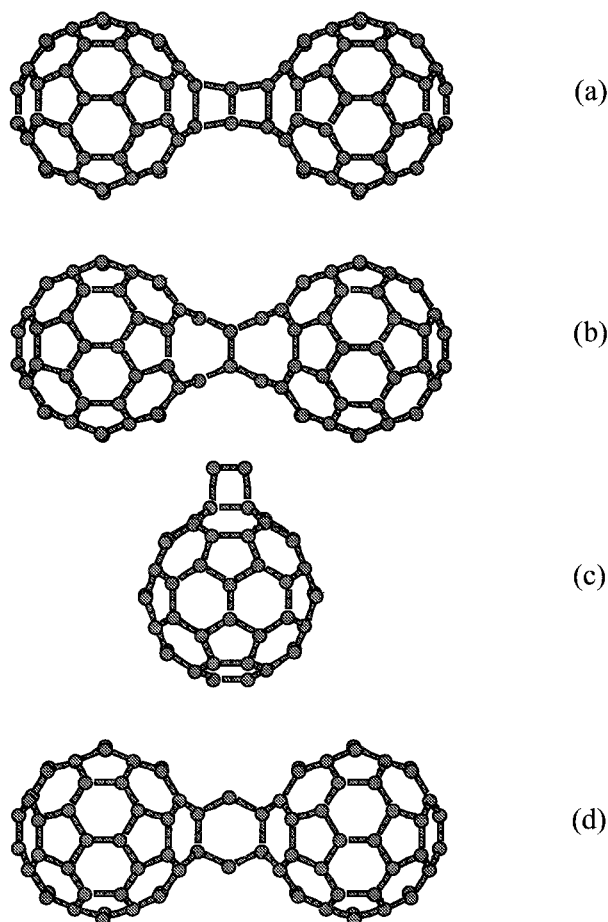
The dimers involving C_{70} have not been optimized, again owing to the exceedingly large number of possible isomers. Indeed, C_{70} has five symmetry-distinct atoms and eight different bonds. This allows for 5 inequivalent sp and up to 16 sp^2 joints to a chain, which could add to C_{60} producing 5 sp and up to 60 sp^2 dimers, not including enantiomers and mixed sp/sp^2 species. However, we note that the positions of new peaks observed for cations and anions of $n = 132-136$ relative to the [2 + 2] cycloadducts are exactly the same as for C_{n-10} (compare Figure 2 vs Figure 1). This and the other commonalities in behavior described in the experimental section above provide convincing evidence for the assignment of the rightmost significant features in the drift time distributions for $n = 132-136$ to the $(C_{60}-chain-C_{70})$ structures. For $C_{142}-C_{146}$, broad featureless tails on the right sides of [2 + 2] cycloadducts may be due to the unresolved ball-and-chain dimers and/or tailed geometries. Hundreds of ball-and-chain dimer isomers possible in the systems involving two C_{70} fullerenes may readily convolute into such tails.

Special Behavior of C_{122} and C_{132}. Both cation and anion for $n = 122$ and 132 exhibit a major peak immediately to the right of [2 + 2] cycloadducts. The analysis of this feature below is for $n = 122$; the discussion would mostly apply to $n = 132$ upon substituting C_{70} for one C_{60}. The peak in question is more abundant than the ball-and-chain dimers, especially for the cation. Its abundance actually exceeds that of any other new structure revealed here for any size and charge state. The measured drift times are too short for any ball-and-chain dimers, and in any event this would not explain the singularity for $n = 122$. On the other hand, these times are too long for the singly bonded $C_{60} \cdot C_{62}$ adducts[57] analogous to that shown in Figure 4. A tailed dimer with a C−C unit attached opposite to the [2 + 2] link on $C_{60} \cdot C_{60}$ fits the measured mobilities. There is, however, no reason for the tailed dimers to exist for $n = 122$ only, particularly in the absence of such geometries with different chain attachment sites (such as in Figure 6b) that would fill the gap in mobilities between the [2 + 2] cycloadducts and the discussed feature.[58] The inordinate yield of this moiety suggests that it is built from the original fullerenes and C_2, the two molecules most ubiquitous in the hot fullerene plasma. The cages could be linked either directly or via C_2. A direct addition would produce a tailed dimer, which is unlikely as outlined above.

The only option[59] to connect two fullerenes using C_2 other than constructing a ball-and-chain dimer is to sandwich C_2 between them in a "double [2 + 2] cycloadduct" akin to the standard [2 + 2] $(C_{60})_2$ or $C_{60} \cdot C_{70}$. As in the sp^2 adducts discussed above, the hinge bond could be either closed (Figure 8a) or open (Figure 8b). For C_{122}, a 56 or 66 site could be involved on each fullerene. We calculate the closed-66/66 adduct in Figure 8a to be lower in energy than the closed-56/56 one by 1.6 eV for the neutral and 1.2 eV for cation or anion.[60] This is exactly like $(C_{60})_2$, where the neutral 66/66 isomer is lower than the 56/56 or 56/65 one by 1.6 eV. The strained hinge bond in closed-56/56 double [2 + 2] may sever, resulting in the nearly isoenergetic open-56/56 adduct.[60] However, the open-66/66 isomer in Figure 8b is extremely unfavorable; it lies ~3.8 eV above the closed geometry in AM1 and is not even a local minimum in DFTB.

The closed-66/66 C_{122} is essentially degenerate with the sp ball-and-chain geometry (the difference being ±0.4 eV depending on the charge) in DFTB and below it by 1.2 eV in AM1. The mobility calculated for either 56/56 or 66/66 double [2 + 2] adducts (particularly the "open" ones) is closer to the measurements for both cation and anion than any of the ball-and-chain dimers (see Figure 1). The species in Figure 8a could readily form by a [2 + 2] cycloaddition of C_2 to a double bond on C_{60}, creating a "handle" (Figure 8c) and subsequent [2 + 2] addition of another C_{60} satisfying the dangling bonds on this handle.[61] This naturally explains why this structure is unique for $n = 122$; C_4 and longer chains can attach one end to a fullerene, forming tadpoles, but cannot lie flat on the fullerene surface. The dissociation energy calculated for this double [2 + 2] is 3.4 eV for the cation, 2.8 eV for the neutral (2.9 eV in

Conclusions

We have now completed a detailed investigation of the structure of clusters comprising the wide mass envelopes of "dimers" produced by laser desorption of C_{60} and C_{70}. We found that the species with masses equal to or less than double the original fullerene (C_k) mass are fully coalesced near-spherical cages and [2 + 2] cycloadducts,[18,19] the abundance of the former increasing with increasing laser power. These two series also dominate the isomer distributions for C_n species heavier than the exact dimers ($n > 2k$). However, there appears to be a new family of ball-and-chain dimers with fullerenes linked by linear chains up to eight atoms long. These adducts mostly involve the original cages, but dimers comprising smaller or larger fullerenes also exist. The C_{2k+2} clusters present a special case, with a substantial abundance of isomer consisting of a C_2 unit sandwiched between two original fullerenes. Multiply bound geometries proposed in the literature have not been observed for any nuclearity.

This information sketches the chemical processes in hot fullerene plasma as follows. Fullerenes in a plume desorbed by a laser have widely different internal temperatures, depending on their position with respect to the laser spot on the film and other factors. Once in the gas phase, all clusters are cooled by He at near-ambient conditions. So what happens to a particular molecule depends on its initial temperature and the cluster density in its vicinity that determines the probability of collisions before the mixture composition is frozen out. Some fullerenes are so hot that they rapidly undergo one or more successive steps of C_2 elimination (shrinking), each reducing the internal energy by ≥ 10 eV.[61,62] The C_2 neutrals thus produced join easily, creating longer chains. They also add to fullerenes of all sizes by incorporation into the wall, making larger cages, and by addition to the double bonds forming "handles". Chains of any length attach to all fullerenes creating tadpoles. These can lengthen the dangling bond by adding further chains and tie it up by attaching other fullerenes or tadpoles to create ball-and-chain dimers. Handles similarly terminate the dangling bonds on the handle by adding another fullerene. One tadpole could conceivably attach to the cage of another, leaving a dangling bond on the latter. We have, however, not observed such geometries in significant abundance presumably because the population of tadpoles is low enough to make their collisions improbable or because these dimers easily undergo further additions at the dangling bond.

Some fullerenes are not hot enough to shrink before being cooled by He but can, together with another cage, surmount the potential barrier of only ~1.5 eV to dimerization into [2 + 2] cycloadducts.[19] This fullerene may be pristine C_{60}, a smaller cage cooled by evaporation or a larger one produced by C_2 incorporation. The most excited of the dimers jump over another barrier of ~1.5 eV and, after descending a ladder of intermediates with decreasing center-to-center distance, anneal into the global minimum of the system: near-spherical cages.[19] The rest are trapped out in the metastable [2 + 2] cycloadducts or elongated buckytubes. The isomerization of a [2 + 2] cycloadduct into a giant fullerene releases over 20 eV, which may cause the produced cage to shrink, ejecting more C_2.[19] Of course, these secondary C_2 may feed into all the reactions listed above for primary C_2 arising from the dissociation of laser-heated original fullerene. Tadpoles could also participate in the [2 + 2] cycloadditions, and chains may add to the [2 + 2] dimers. Both these processes form tailed dimers that are likely responsible for the decaying tails on the right sides of [2 + 2] cycloadduct peaks in our experiments.

Figure 8. (a) "Double [2 + 2]" closed-66 isomer for C_{122} analogous to the $(C_{60})_2$ [2 + 2] cycloadduct. (b) Open-66 analogue of (a). (c) "Handle" C_{62} geometry postulated as the precursor to (a). (d) C_{122} with the "benzene" link.

AM1), and 2.7 eV for the anion. So this cluster is as stable to fragmentation as any C_{122} ball-and-chain dimer and much more stable than the sp isomer.

One could think of a C_{122} with the "benzene" link (Figure 8d). Its mobility agrees with the data better than that of a double [2 + 2] cycloadduct. Unfortunately, the energy of this local minimum in all charge states is substantially higher (by 4.0–4.6 eV in DFTB and 3 eV in AM1) than that of the structure in Figure 8a. There also is no clear route for this cluster to form under our conditions. (It could hardly form directly because single carbon atoms are not a major component of the reactant mixture. In principle, it could be produced by severing the bond between two carbons in the middle of double [2 + 2], but this is implausible in view of high activation energy involved.) So, while the peak for C_{122} and C_{132} immediately to the right of [2 + 2] cycloadducts is likely to be due to a C_2 squashed between two fullerenes, the precise geometry is not entirely clear. We presently continue to research this matter as a part of our study of fullerene tadpoles.[59]

Similar to the case of [2 + 2] fullerene cycloadducts,[18,19] the correct evaluation of mobilities for ball-and-chain dimers is contingent on carrying out the trajectory calculations that account for the multiple scattering of helium atoms on the concave part of dimer surface.[30] The projection approximation[45] ignores this effect. This results in the underestimation of collision integrals for the ball-and-chain dimers by ~5%, which would have rendered all the structural assignments made above impossible.

This picture explains the patterns in ball-and-chain dimer abundances. First, such dimers containing C_{60} or C_{70} only are probably not preferable to those involving other cages, and a particular prominence of the former follows from the great abundance of the original fullerene in comparison with neighboring sizes apparent in the mass spectrum. Similarly, the decreasing intensity of ball-and-chain dimers for longer chains is hardly related to the intrinsic stability of dimers. Although the calculated dissociation energies of these species decrease with increasing chain length in all charge states (Table 1), this alone would not suffice in explanation because the absolute values are still above the activation barriers for the dissociation of [2 + 2] cycloadducts even for $n = 128$. The abundances of ball-and-chain dimers simply reflect the availability of reactants. Indeed, for the chains lengthening by accretion of C_2 units onto chains (whether free or attached to fullerenes in tadpoles), the probability of encountering a specific chain is anticorrelated with its length. This means that the yield of ball-and-chain dimers in general, but particularly of those with longer chains, could be enhanced by seeding the reacting plasma with chains, for example, by covaporization of graphite as in the setup of Martin and co-workers.[27] Chains as long as ∼15 atoms for the neutral[63,64] and ∼50 atoms for the anion[31,46] have been produced in this way under conditions resembling those in our source. So the ball-and-chain dimers with much greater distances between the fullerenes could likely be made.

This research has been largely driven by the unique position that the fullerene-based species occupy in cluster science. That is, most of them first characterized in the gas phase have been subsequently synthesized and isolated in bulk. This applies to C_{60} itself,[65,66] other fullerenes,[65,67] endohedral complexes,[68,69] C_{119},[70,71] and most recently, the [2 + 2] C_{60} dimer.[18,21,22] The first ball-and-chain dimer (C_{122}) has already been isolated,[25,26] and it is hoped that others reported here would be too.

References and Notes

(1) Rao, A. M.; Zhou, P.; Wang, K. A.; Hager, G. T.; Holden, J. M.; Wang, Y.; Lee, W. T.; Bi, X. X.; Eklund, P. C.; Cornett, D. S.; Duncan, M. A.; Amster, I. J. *Science* **1993**, *259*, 955.

(2) Cornett, D. S.; Amster, I. J.; Duncan, M. A.; Rao, A. M.; Eklund, P. C. *J. Phys. Chem.* **1993**, *97*, 5036.

(3) Eklund, P. C.; Rao, A. M.; Zhou, P.; Wang, Y.; Wang, K. A.; Holden, J. M.; Dresselhaus, M. S.; Dresselhaus, G. *Mol. Cryst. Liq. Cryst.* **1994**, *256*, 199.

(4) Eklund, P. C.; Rao, A. M.; Zhou, P.; Wang, Y.; Holden, J. M. *Thin Solid Films* **1995**, *257*, 185.

(5) Rao, A. M.; Eklund, P. C. *Mater. Sci. Forum* **1996**, *232*, 173.

(6) Rao, A. M.; Eklund, P. C.; Venkateswaran, U. D.; Tucker, J.; Duncan, M. A.; Bendele, G. M.; Stephens, P. W.; Hodeau, J. L.; Marques, L.; Nunez-Regueiro, M.; Bashkin, I. O.; Ponyatovsky, E. G.; Morovsky, A. P. *Appl. Phys. A* **1997**, *64*, 231.

(7) Beck, R. D.; Weis, P.; Brauchle, G.; Kappes, M. M. *J. Chem. Phys.* **1994**, *100*, 262.

(8) Yeretzian, C.; Hansen, K.; Diederich, F.; Whetten, R. L. *Nature* **1992**, *359*, 44. Yeretzian, C.; Hansen, K.; Diederich, F.; Whetten, R. L. *Z. Phys. D* **1993**, *26*, S300.

(9) Hansen, K.; Yeretzian, C.; Whetten, R. L. *Chem. Phys. Lett.* **1994**, *218*, 462.

(10) Ata, M.; Takahashi, N.; Nojima, K. *J. Phys. Chem.* **1994**, *98*, 9960.

(11) Takahashi, N.; Dock, H.; Matsuzawa, N.; Ata, M. *J. Appl. Phys.* **1993**, *74*, 5790.

(12) Ulmer, G.; Campbell, E. E. B.; Kuhnle, R.; Busmann, H. G.; Hertel, I. V. *Chem. Phys. Lett.* **1991**, *182*, 114.

(13) Mitzner, R.; Winter, B.; Kusch, Ch.; Campbell, E. E. B.; Hertel, I. V. *Z. Phys. D* **1996**, *37*, 89.

(14) Rao, A. M.; Menon, M.; Wang, K. A.; Eklund, P. C.; Subbaswamy, K. R.; Cornett, D. S.; Duncan, M. A.; Amster, I. J. *Chem. Phys. Lett.* **1994**, *224*, 106.

(15) Menon, M.; Rao, A. M.; Subbaswamy, K. R.; Eklund, P. C. *Phys. Rev. B* **1995**, *51*, 800.

(16) Ata, M.; Kurihara, K.; Takahashi, N. *J. Phys. Chem. B* **1997**, *101*, 5.

(17) Hunter, J. M.; Fye, J. L.; Boivin, N. M.; Jarrold, M. F. *J. Phys. Chem.* **1994**, *98*, 7440.

(18) Shvartsburg, A. A.; Hudgins, R. R.; Dugourd, Ph.; Jarrold, M. F. *J. Phys. Chem. A* **1997**, *101*, 1684.

(19) Shvartsburg, A. A.; Pederson, L. A.; Hudgins, R. R.; Schatz, G. C.; Jarrold, M. F. *J. Phys. Chem. A* **1998**, *102*, 7919.

(20) Fowler, P. W.; Mitchell, D.; Taylor, R.; Seifert, G. *J. Chem. Soc., Perkin Trans. 2* **1997**, 1901.

(21) Wang, G. W.; Komatsu, K.; Murata, Y.; Shiro, M. *Nature* **1997**, *387*, 583.

(22) Lebedkin, S.; Gromov, A.; Giesa, S.; Gleiter, R.; Renker, B.; Rietschel, H.; Kratschmer, W. *Chem. Phys. Lett.* **1998**, *285*, 210.

(23) Ueno, H.; Osawa, S.; Osawa, E.; Takeuchi, K. *Fullerene Sci. Technol.* **1998**, *6*, 319.

(24) Osterodt, J.; Vogtle, F. *Chem. Commun.* **1996**, 547.

(25) Fabre, T. S.; Treleaven, W. D.; McCarley, T. D.; Newton, C. L.; Landry, R. M.; Saraiva, M. C.; Strongin, R. M. *J. Org. Chem.* **1998**, *63*, 3522.

(26) Dragoe, N.; Tanibayashi, S.; Nakahara, K.; Nakao, S.; Shimotani, H.; Xiao, L.; Kitazawa, K.; Achiba, Y.; Kikuchi, K.; Nojima, K. *Chem. Commun.* **1999**, 85.

(27) Tast, F.; Malinowski, N.; Billas, I. M.; Heinebrodt, M.; Branz, W.; Martin, T. P. *J. Chem. Phys.* **1997**, *107*, 6980.

(28) Dugourd, Ph.; Hudgins, R. R.; Clemmer, D. E.; Jarrold, M. F. *Rev. Sci. Instrum.* **1997**, *68*, 1122.

(29) Mason, E. A.; McDaniel, E. W. *Transport Properties of Ions in Gases*; Wiley: New York, 1988.

(30) Mesleh, M. F.; Hunter, J. M.; Shvartsburg, A. A.; Schatz, G. C.; Jarrold, M. F. *J. Phys. Chem.* **1996**, *100*, 16082. Mesleh, M. F.; Hunter, J. M.; Shvartsburg, A. A.; Schatz, G. C.; Jarrold, M. F. *J. Phys. Chem. A* **1997**, *101*, 968.

(31) Shvartsburg, A. A.; Schatz, G. C.; Jarrold, M. F. *J. Chem. Phys.* **1998**, *108*, 2416.

(32) Dugourd, Ph.; Hudgins, R. R.; Tenenbaum, J. M.; Jarrold, M. F. *Phys. Rev. Lett.* **1998**, *80*, 4197.

(33) Elstner, M.; Porezag, D.; Jungnickel, G.; Elsner, J.; Haugk, M.; Frauenheim, Th.; Suhai, S.; Seifert, G. *Phys. Rev. B* **1998,** *52*, 7260.

(34) Porezag, D.; Frauenheim, Th.; Kohler, Th.; Seifert, G.; Kaschner, R. *Phys. Rev. B* **1995**, *51*, 12947.

(35) Ayuela, A.; Fowler, P. W.; Mitchell, D.; Schmidt, R.; Seifert, G.; Zerbetto, F. *J. Phys. Chem.* **1996**, *100*, 15634.

(36) Fowler, P. W.; Heine, T.; Manolopoulos, D. E.; Mitchell, D.; Orlandi, G.; Schmidt, R.; Seifert, G.; Zerbetto, F. *J. Phys. Chem.* **1996**, *100*, 6984.

(37) Fowler, P. W.; Heine, T.; Mitchell, D.; Orlandi, G.; Schmidt, R.; Seifert, G.; Zerbetto, F. *J. Chem. Soc., Faraday Trans.* **1996**, *92*, 2203.

(38) Porezag, D.; Pederson, M. R.; Frauenheim, Th.; Köhler, Th. *Phys. Rev. B* **1995**, *52*, 14963.

(39) Porezag, D.; Jungnickel, G.; Frauenheim, Th.; Seifert, G.; Ayuela, A.; Pederson, M. R. *Appl. Phys. A* **1997**, *64*, 321.

(40) Kürti, J.; Németh, K. *Chem. Phys. Lett.* **1996**, *256*, 119.

(41) Stafström, S.; Fagerström, J. *Appl. Phys. A* **1997**, *64*, 307.

(42) Matsuzawa, N.; Ata, M.; Dixon, D. A.; Fitzgerald, G. *J. Phys. Chem.* **1994**, *98*, 2555.

(43) Osawa, S.; Osawa, E.; Hirose, Y. *Fullerene Sci. Technol.* **1995**, *3*, 565.

(44) Osawa, S.; Sakai, M.; Osawa, E. *J. Phys. Chem. A* **1997**, *101*, 1378.

(45) Von Helden, G.; Hsu, M. T.; Gotts, N.; Bowers, M. T. *J. Phys. Chem.* **1993**, *97*, 8182.

(46) Gotts, N. G.; von Helden, G.; Bowers, M. T. *Int. J. Mass Spectrom. Ion Processes* **1995**, *149/150*, 217.

(47) Scuseria, G. E. *Chem. Phys. Lett.* **1996**, *257*, 583.

(48) Strout, D. L.; Murry, R. L.; Xu, C.; Eckhoff, W. C.; Odom, G. K.; Scuseria, G. E. *Chem. Phys. Lett.* **1993**, *214*, 576.

(49) Ho, K. M.; Shvartsburg, A. A.; Pan, B. C.; Lu, Z. Y.; Wang, C. Z.; Wacker, J. G.; Fye, J. L.; Jarrold, M. F. *Nature* **1998**, *392*, 582.

(50) Wang, Y.; Holden, J. M.; Bi, X. X.; Eklund, P. C. *Chem. Phys. Lett.* **1994**, *217*, 413.

(51) Patchkovskii, S.; Thiel, W. *J. Am. Chem. Soc.* **1998**, *120*, 556.

(52) Hunter, J. M.; Jarrold, M. F. *J. Am. Chem. Soc.* **1995**, *117*, 10317.

(53) All fullerene dimer features for anions are encountered in the measurements at drift times ∼0.6% longer than those for cations. This also

occurs for C_{60} and other fullerenes with $n \approx 60$. We have ascertained that the geometric difference between C_{60}^+ [54] and C_{60}^- [55] is far too small to cause this effect. So it is probably due to a marginal expansion of the electronic cloud on which the He atoms actually scatter. Since our C−He interaction potential has been fit for C_{60}^+,[30] we correct the calculated collision integrals by 1.006 when comparing them with the measurements for anions.

(54) Bendale, R. D.; Stanton, J. F.; Zerner, M. C. *Chem. Phys. Lett.* **1992**, *194*, 467.

(55) Green, W. H.; Gorun, S. M.; Fitzgerald, G.; Fowler, P. W.; Ceulemans, A.; Titeca, B. C. *J. Phys. Chem.* **1996**, *100*, 14892.

(56) We could not determine if this feature is present for C_{128}^- because of insufficient signal.

(57) Estimated using the measured or calculated mobilities for C_{62} and the value computed for singly bonded C_{60} dimer.[18] The results are independent of whether C_{62} is a fullerene or the nonclassical heptagon-containing cage discovered by Ayuela et al.[35]

(58) In the absence of thermodynamic or kinetic preference, the abundance of other regioisomers should be many times larger simply because of the relative number of sites available for addition at ∼90° and ∼180° to the [2 + 2] link. The gap between [2 + 2] cycloadducts and the discussed feature is not as clear for $n = 132$, but this is probably due to the broadening of both peaks by the large number of regioisomers with slightly differing mobilities that exist for the dimers including C_{70}.

(59) Shvartsburg, A. A.; et al. To be published.

(60) In AM1, the double [2 + 2] C_{122} with 56 hinge bonds closed is unstable and relaxes to the "open" geometry.

(61) Murry, R. L.; Strout, D. L.; Odom, G. K.; Scuseria, G. E. *Nature* **1993**, *366*, 665.

(62) Hansen, K.; Echt, O. *Phys. Rev. Lett.* **1997**, *78*, 2337.

(63) Lee, S.; Gotts, N.; von Helden, G.; Bowers, M. T. *J. Phys. Chem. A* **1997**, *101*, 2096.

(64) Giesen, T. F.; Van Orden, A.; Hwang, H. J.; Fellers, R. S.; Provencal, R. A.; Saykally, R. J. *Science* **1994**, *265*, 756.

(65) Kroto, H. W.; Heath, J. R.; O'Brien, S. C.; Curl, R. F.; Smalley, R. E. *Nature* **1985**, *318*, 162.

(66) Krätschmer, W.; Lamb, L. D.; Fostiropoulos, K.; Huffman, D. R. *Nature* **1990**, *347*, 354.

(67) Taylor, R.; Hare, J. P.; Abdul-Sada, A. K.; Kroto, H. W. *Chem. Commun*. **1990**, 1423.

(68) Heath, J. R.; O'Brien, S. C.; Zhang, Q.; Liu, Y.; Curl, R. F.; Kroto, H. W.; Tittel, F. K.; Smalley, R. E. *J. Am. Chem. Soc.* **1985**, *107*, 7779.

(69) Chai, Y.; Guo, T.; Jin, C.; Haufler, R. E.; Chibante, L. P. F.; Fure, J.; Wang, L.; Alford, J. M.; Smalley, R. E. *J. Phys. Chem.* **1991**, *95*, 7564.

(70) McElvany, S. W.; Callahan, J. H.; Ross, M. M.; Lamb, L. D.; Huffman, D. R. *Science* **1993**, *260*, 1632.

(71) Gromov, A.; Ballenweg, S.; Giesa, S.; Lebedkin, S.; Hull, W. E.; Krätschmer, W. *Chem. Phys*. *Lett*. **1997**, *267*, 460.